Distribution of barium in the Weddell Gyre: Impact of circulation and biogeochemical processes

M. Hoppema, F. Dehairs, J. Navez, C. Monnin, C. Jeandel, E. Fahrbach, H. J. W. de Baar

Distribution of barium in the Weddell Gyre: Impact of circulation and biogeochemical processes

M. Hoppema[a,1], F. Dehairs[b], J. Navez[b,c], C. Monnin[d], C. Jeandel[e], E. Fahrbach[a], H.J.W. de Baar[f]

[a] Alfred Wegener Institute for Polar and Marine Research, Climate Sciences Department, Postfach 120161, D-27515 Bremerhaven, Germany

[b] Vrije Universiteit Brussel, Earth System Sciences & Analytical and Environmental Chemistry, Pleinlaan 2, B-1050 Brussels, Belgium

[c] Royal Museum for Central Africa, Geology and Mineralogy - Section of Mineralogy and Petrography, Leuvensesteenweg, B-3080 Tervuren, Belgium

[d] Laboratoire Mécanismes de Transfert en Géologie, CNRS/Université Paul Sabatier, 16 Avenue Edouard Belin, F-31400 Toulouse, France

[e] Laboratoire d'Etudes en Géophysique et Océanographie Spatiales (LEGOS), Observatoire Midi Pyrénées, F-31400 Toulouse, France

[f] Royal Netherlands Institute for Sea Research, Postbus 59, NL-1790 AB Texel, the Netherlands

[1] corresponding author: Mario.Hoppema@awi.de ; phone +49 471 48311884

Email F. Dehairs: fdehairs@vub.ac.be

Key words : Barium; silicate; geochemical cycle; (Southern Ocean, Weddell Sea)

Abstract

The Southern Ocean data base of dissolved barium (Ba_d) has been augmented significantly with two sections across the Weddell Gyre sampled by the icebreaker FS Polarstern during February and March 2005. Ba_d was found to be relatively high in the surface layer as compared to the adjacent waters north (Antarctic Circumpolar Current) and east (Antarctic Zone of the Indian sector). Compared to the inflowing water into the Weddell Gyre and also to the surface water, the deep water is characterized by a Ba_d enrichment. We identified sea-ice formation as a further process, besides well-known biogeochemical processes, that leads to the extraction of Ba from solution via barite ($BaSO_4$) precipitation. The particles rain down the water column and redissolve in deeper water where undersaturation of barite is prevalent. In the bottom layer, an enhanced enrichment of Ba_d occurs, exhibited as a Ba_d maximum, which is caused by Ba efflux from the sediments. In recently formed Weddell Sea Bottom Water, though, a Ba_d minimum is observed, imposed by the shelf water component of bottom water, which has relatively low Ba_d concentration. Like in other Southern Ocean regions, all through the water column a strong correlation exists between Ba_d and dissolved silicate, although the relationship is different from that in the Antarctic regions to the east. The Weddell Gyre appears to be a source of Ba_d to the deep and abyssal world oceans via Antarctic Bottom Water export. The aforementioned mechanism of barite precipitation accompanying sea ice formation and subsequent redissolution in the deep Weddell is a main factor in this.

Introduction

The distribution of barium (Ba) in the ocean is not only controlled by water mass mixing, but also by biologically-mediated uptake followed by dissolution (Chan et al., 1977; Jeandel et al. 1996). These conditions impose that Ba be categorized as a bio-intermediate element. This fits ~~in~~ the picture that higher biomass and productivity in the upper mixed layer usually coincide with higher Ba concentrations in suspended matter (e.g., Cardinal et al., 2005; Jacquet et al., 2007a). Most of this upper mixed layer particulate, non-lithogenic Ba is not yet in the form of the compound barite, but rather consists of Ba absorbed by or adsorbed on planktonic material (Cardinal et al., 2005; Jacquet et al. 2007b, 2008~~a~~). Apart from Fresnel et al. (1979), we are not aware of any other study reporting the presence of barite in living marine phytoplankton. However, freshwater and marine benthic microbial organisms have been reported to be associated with barite (e.g., Hopwood et al., 1997; Bertram and Cowen, 1997). For the water

column underneath the surface mixed layer it is well established that barite is the major carrier of Ba in suspended matter (Dehairs et al., 1980; Jacquet et al., 2007b; Stroobants et al., 1991). Barite formation has been demonstrated to be associated with degradation of phytoplankton material (Ganeshram et al., 2003). This process occurs essentially below the mixed layer in the mesopelagic zone (100-1000 m) within aggregates of decomposing organic detritus (Cardinal et al., 2005; Dehairs et al., 1980, 1990; Stroobants et al., 1991). These subsurface particulate Ba-barite stocks were observed to be correlated with oxygen consumption rates (Dehairs et al., 1997) and more recently evidence was found that mesopelagic excess Ba, or barite is correlated with subsurface bacterial activity (Dehairs et al., 2008; Jacquet et al., 2008a).

The present study explores the distribution of dissolved Ba and silicate in the water column of the Weddell Gyre, an area for which there is a dearth of data on Ba, despite its importance in terms of formation of ventilated deep and bottom water, upwelling and sea-ice formation. Earlier data for the Weddell region were obtained during the GEOSECS project but they consist only of few full-depth profiles and some surface plus bottom water only data (Chan et al., 1977; Östlund et al., 1987). Expedition ANT-XXII/3 in 2005 offered the possibility to investigate Ba along the Prime Meridian and at a section across the Weddell basin (Fig. 1), thereby significantly expanding the Southern Ocean data set which thus far consists of sections along 30°E (WOCE I6; Dehairs et al., unpublished results) and 145°E (WOCE SR3; Jacquet et al., 2004).

Material and methods

Data were collected (Fig. 1) during FS Polarstern cruise ANT-XXII/3 from Cape Town, South Africa to Punta Arenas, Chile, 22 January to 6 April 2005 (Fahrbach, 2006). Water was sampled with the rosette sampler coupled to the CTD instrument (conductivity temperature depth; SBE911plus) all through the water column, with a bias to the upper 1000 m. Temperature and salinity were measured with a precision of 0.001°C and 0.002, respectively (Fahrbach, 2006).

Dissolved barium

Volumes of 15 ml of unfiltered seawater were sampled in polypropylene vials (Nalgene), which were rinsed three times with the sample seawater. Samples were acidified with 15 µl

HCl (Merck Suprapur) and stored at room temperature until analysis in the home laboratory. No filtration of the seawater was attempted based on the well documented knowledge that dissolved Ba represents in general a very large fraction (> 99%) of total Ba. In productive surface mixed layers this may be different but also here particulate Ba is usually <3% of total Ba (~~see e.g.,~~ Jacquet et al., 2007a; 2008). Dissolved Ba was measured using an isotope dilution method described below; in fact it constitutes ~~dissolvable~~ Ba, consisting of dissolved Ba plus a very small fraction (generally <1% of total Ba) that is generated from the particulate Ba pool as a result of the acidification. For the sake of simplicity we prefer to use the term dissolved Ba in this manuscript. Sample preparation is as follows: 1 g of seawater is spiked with 0.7 g of ^{135}Ba-spike solution yielding a ^{138}Ba/^{135}Ba ratio between 0.7 and 1 to minimize error propagation (Webster, 1960; Klinkenberg et al., 1996). Subsequently the sample is diluted with Milli-Q grade water to a final weight of 30 g. Blanks consist of acidified (nitric acid) Milli-Q water. Quantities of sample, spike and dilution water were accurately assessed by weighing. Isotope ratios were measured with a SF-ICP-MS (Element 2 Thermo Finnigan). Reproducibility of our method is ± 1.5% (RSD) as tested on repeat preparations of reference solutions. Average Ba values obtained for reference waters SLRS-3 and an in-house standard (a Mediterranean Sea standard prepared by C. Jeandel) were 13.48 ± 0.21 µg l^{-1} (1σ) with RSD of 1.55% and 10.49 ± 0.29 µg l^{-1} (1σ) with RSD of 2.75%, respectively, which is in good agreement with certified values (SLRS-3: 13.4 ± 0.6 µg l^{-1} and OMP: 10.4 ± 0.2 µg l^{-1}). Overall precision (including sampling precision) based on 6 dissolved Ba profiles sampled in a hydrographically stable environment is ± 0.3 µg l^{-1} (1σ) with an RSD of 5% (Dehairs et al., 2008; Jacquet, 2007); for further details we refer to the latter two studies. Ba_d concentrations are expressed in nmol kg^{-1}.

Silicate

Nutrients were measured on board with a Technicon TRAACS 800 rapid flow autoanalyzer (see also Fahrbach, 2006) by the Royal Netherlands Institute for Sea Research (NIOZ, Texel). Accuracy was determined using stock standards diluted in low-nutrient sea water, as prepared in the home lab by weighing. The precision for silicate was estimated to be 0.66 µmol l^{-1} at two calibration stations, where all 24 rosette bottles were fired at the same depth. Part of the surface layer nutrient data of this cruise have also been reported by Hoppema et al. (2007). Silicate (or silicic acid) concentrations are expressed in µmol kg^{-1}.

$BaSO_4$ saturation index calculation

The barite saturation index (SI) is defined as the ratio of the ionic product of barium sulfate (Q) to the solubility product of barite (K_{sp}).

$$SI = \frac{Q}{K_{sp}} = \frac{m_{Ba(aq)} \cdot m_{SO_4(aq)} \cdot \gamma^2_{BaSO_4(aq)}}{K_{sp}} \qquad (1)$$

in which m is the measured concentration (molality) and γ the activity coefficient of aqueous barium sulfate. Monnin (1999) has developed a model of the Na-K-Ca-Mg-Sr-Ba-Cl-SO_4-H_2O system that allows the calculation of the solubility and saturation indices of some minerals, including barite, as a function of the solution composition, temperature (up to 200°C) and pressure (up to 1 kbar). It has been used to investigate the saturation state of the ocean with respect to pure barite (Monnin et al., 1999) and Sr-substituted barites (Monnin and Cividini, 2006). The criterion for equilibrium retained in these studies is a saturation index between 0.9 and 1.1, which has been inferred from an evaluation of the mean accuracy of the solubility calculations during model development (Monnin, 1999). The measured quantities used are dissolved barium molarity, salinity, pressure and potential temperature. The concentrations of Na, K, Ca, Mg, Ba, Cl, SO_4 and Cl are calculated from the measured salinity and the composition of standard seawater of salinity 35 using:

$$c_i(S) = c_i(35) \times \frac{S}{35} \qquad (2)$$

with $c_i(S)$ the concentration (molarity) of the i^{th} element for the sample with salinity S. The Na concentration is calculated from the electroneutrality condition. Molarities are converted to molalities using the VOlumetric_PrOperties (VOPO) code (Monnin 1994). The thermodynamic model then calculates the stoichiometric $BaSO_4$(aq) activity coefficient, the barite solubility product and the barite saturation index at the given temperature and pressure.

Hydrographic background

The region of investigation is situated in the Antarctic Zone, i.e. south of the Polar Front. The boundary between the Antarctic Circumpolar Current (ACC) and the Weddell Gyre can be identified at about 56°S on the Prime Meridian (Klatt et al., 2005). Thus the majority of data stem from the Weddell ~~regime~~. North of 56°S the potential temperature maximum of the Upper Circumpolar Deep Water (UCDW) can be distinguished, centered at 500-600 m (Fig. 2). Circumpolar Deep Water (CDW) characterized by a maximum in the potential temperature (θ) is transferred into the Weddell Gyre near its eastern end. We observed the temperature maximum at 64-69°S ~~in~~ 150-400 m depth reaching 0.8-1°C (Fig. 2); this coincides essentially with the westward flowing southern limb of the Weddell ~~Gyre – note~~ that the θ maximum layer is interrupted near 66°S by a lower θ maximum around the undersea mountain Maud Rise. At the northern part (56-63.5°S) of the Prime Meridian section, constituting the northern limb of the gyre with generally eastward flow, a θ maximum was observed as well, but it reaches only about 0.5°C (Fig. 2). This is CDW which has been modified by mixing with waters above and below during its course through the Weddell Gyre. The θ maximum layer is separated from the base of the surface layer (identified by a temperature minimum) by a sharp pycnocline. In the upper part of the surface layer, temperatures were often >1.0 °C, but in the coastal region it was significantly colder. These are summer temperatures; in winter the entire surface layer is at or close to the freezing point of about -1.85°C. Note that the surface layer is deeper in the coastal zone than elsewhere in the basin. The Weddell Gyre is a divergent feature with upwelling of deep water, mainly more or less modified CDW; the surface layer is eventually generated from this upwelled water. In the deep Weddell basin, θ decreases monotonically from the θ max to a minimum at the sea floor. Weddell Sea Bottom Water (WSBW) is present along the section, being defined by θ < –0.7°C. Between the lower boundary of the CDW at 0°C and the WSBW, the most voluminous water mass of the Weddell Gyre is found, the Weddell Sea Deep Water (WSDW). It is replenished by upward mixing of WSBW with CDW, by local water mass formation processes (Orsi et al., 1993), but also by advective transport from the east (Meredith et al. 2000; Hoppema et al., 2001).

Results

The most conspicuous feature in the Ba_d distribution is the difference between the upper 500-1000 m and the deep basin (Fig. 3), which is similar to the θ distribution (Fig. 2).

Concentrations below about 500-1000 m ~~are~~ mainly ~~ranging~~ between 90 and 105 nmol kg^{-1}, which appears to be the background level of Ba_d of the deep Weddell-Enderby basin. At the Prime Meridian, Ba_d concentrations in the deep basin (>1000 m) appear to be highest in the central part (Fig. 3A), reaching up to 107 nmol kg^{-1} between 2000 and 3000 m at 61.5°S. Over the seamount Maud Rise (65-66°S) and over the northernmost part of the Weddell Gyre (56-58°S) deep and bottom water Ba_d concentrations are the lowest. Further south, between Maud Rise and the Antarctic margin (67-68°S), Ba_d in the bottom layer is again slightly higher (up to 100 nmol kg^{-1}). In the deep Weddell Sea (Fig. 3B; below 1000 m) the Ba_d concentration range is 84-104 nmol kg^{-1}, with lowest values in the western part (in the vicinity of the peninsula margin) and highest in the eastern part of the Weddell transect.

The deep waters (i.e. below 200 m in the central part of the section and below 600 m toward the western and the eastern margins of the basin) are separated from an upper layer which has concentrations < 90 nmol kg^{-1}, largely coinciding with the surface mixed layer. Since surface waters of the Weddell Gyre are eventually formed from upwelled deep water, the lower Ba_d contents in surface waters must be the result of non-conservative processes which cause a partial depletion of Ba_d. Between 58° and 65°S at the Prime Meridian, the Ba_d isolines in the upper 500-1000 m exhibit an upward hump, typical of the divergent Weddell Gyre with westward flow in the south and eastward flow in the north, ~~and~~ which is also seen in the distributions of other parameters like θ (Fig. 2) and silicate (see below). As a consequence ~~of this~~, the vertical extent of the Ba_d depleted upper layer is zonally variable, being larger near the northern and southern boundaries of the section. North of 56°S, i.e. outside the Weddell Gyre, the Ba_d depletion zone appears to overlap with the θ maximum core of the UCDW (Fig. 2). As UCDW waters were reported to contain less Ba_d than the deep waters of the Antarctic Zone (Jacquet et al., 2004; Jeandel et al., 1996), this hints that the low Ba_d in the upper water column of the Weddell Gyre could at least partly result from advection of CDW into the Weddell Basin via the westward flowing southern limb of the gyre. It should be appreciated that the front between the ACC and the Weddell Gyre at 56°S also constitutes a divide between the near-surface water with lower Ba_d to the north and waters with higher Ba_d to the south. In the coastal current at the southern end of the Prime Meridian the mixed layer is deep because of convection, mixing and downwelling (see also θ distribution; Fig. 2) which ~~leads also~~ to a deeper penetration of low Ba_d waters. In addition, the Ba_d concentration in the upper few hundred ~~m in~~ the coastal current appears to be lower (about 77 nmol kg^{-1}) than north of it along the section, where it reaches about 85 nmol kg^{-1}. In the area between 64°S and 66.5°S

the Ba_d depletion reaches greater depths than north and south of it. Here Maud Rise exerts influence on the entire water column: As circulation-topography interaction induces a Taylor column over the rise, the mixed layer extends deeper over the crest of Maud Rise than over its flanks.

Along the Weddell Sea section the near-surface layer exhibits similar Ba_d concentrations (Fig. 3B) as observed at the Prime Meridian. At both ends of the section the low-Ba_d layer also extends deeper than in the central part. At the continental shelf break of the Antarctic Peninsula, the low-Ba_d surface layer is linked to a plume of Ba_d depleted water hugging the continental slope until about 4000 m depth. This plume consists of Weddell Sea Bottom Water, which has very recently been formed at the southern and western shelves of the Weddell Sea and which has not yet reached the bottom of the central basin (Fahrbach et al., 2001; Gordon et al., 1993). Since WSBW is a mixing product of CDW and shelf water, it carries the low-Ba_d properties of the latter water mass. In the WSBW at the continental slope the shelf water component is particularly large; on its further way through the Weddell Sea, mixing with adjacent deep waters will reduce the overall contribution of the shelf water component to the WSBW, thus also increasing the Ba_d concentration.

Discussion

The concentrations of Ba_d are generally higher in Weddell Gyre surface waters compared to the Antarctic Zone in the Indian sector of the Southern Ocean (see Jacquet et al., 2005; Jeandel et al., 1996). Such zonal variation is mainly caused by varying upwelling activity of Ba-enriched deep waters southward in the ACC, although zonal differences in phytoplankton activity probably contribute as well. The latter usually is highest in the Subantarctic zone and Polar Frontal Zone to the north and decreases southwards into the Antarctic Zone to increase again in the vicinity of the ice edge (Jochem et al., 1995; Moore et al., 1999; Savoye et al., 2004). Our Weddell data were collected during summer, at the height of the growth season, and thus we expect the impact of biological uptake on Ba_d to have been at its climax. The smaller Ba_d depletions in Weddell surface waters could thus reflect lower production in the Weddell region compared to elsewhere in the ACC. However, it is likely that this smaller apparent Ba_d depletion is in part due to the intensity of upwelling in the divergent Weddell Gyre transferring Ba-enriched waters into the surface layers. Additionally, deep water which is being upwelled into the surface layer appears to have a higher Ba_d concentration in the

Weddell Gyre than in the Antarctic Zone of the Indian sector (~~compare~~ Jacquet et al., 2004; Jeandel et al., 1996).

Correlation between barium and silicate

The distribution of Ba_d, both lateral and vertical, is known to show similarities with that of silicate in several ocean provinces (e.g., Chan et al., 1977; Jacquet et al., 2007a; Jeandel et al., 1996). We explore the occurrence of such a similarity for the Weddell Gyre with the corresponding silicate sections along the Prime Meridian and across the Weddell Sea (Fig. 4).

The vertical profile of silicate in the Weddell Gyre is typical for that of the major nutrients~~,~~ i.e., relatively low concentrations in the surface layer, a maximum at intermediate depth and a decrease towards the sea floor. Frequently a silicate maximum is observed in the bottom layer (Edmond et al., 1979; Hoppema et al., 1998). Our data demonstrate a high agreement between the distributions of silicate and Ba_d in the Weddell Gyre (Figs. 3 and 4). Even the lateral variation of the extent of the surface layer appears to be congruent. This condition is largely due to hydrographic processes such as upwelling and convective overturning of the surface layer.

Newly formed WSBW at the continental slope off Joinville Island can be recognized by its low silicate and Ba_d concentrations (see NW end of the Weddell section; Figs. 3b and 4b). It is intriguing that even the wide, but not very pronounced, silicate minimum at 3000-3500 m emerging from the lower continental slope off Kapp Norvegia (see SE end of the Weddell section; Figs. 3b and 4b) appears to correspond to a Ba_d minimum. This core of ventilated water, characterized by a CFC maximum (Hoppema et al., 2001; Meredith et al., 2000) and thus a large surface water component, originates east of the Weddell Gyre. ~~Obviously~~, just like WSBW from the Weddell Sea, it is characterized by relatively low concentrations of silicate and Ba_d, although the signal has been attenuated ~~on its long way~~ from the region of origin.

The deep silicate maximum (Fig. 4), which is slightly visible in plots of silicate versus salinity (Fig. 5) is caused by dissolution of biogenic silica at depth (Rutgers van der Loeff and Van Bennekom, 1989). There is no clear ~~coinciding~~ Ba_d maximum - the variability of Ba_d in the deep Weddell Gyre appears too large - although the Ba_d data from the Weddell section seem to point to a weak feature (Fig. 5). Differences between the deep distributions of silicate and

Ba_d should not be surprising, because the saturation state of ocean waters with respect to silica/opal and $BaSO_4$ is different, ~~as well as~~ the dissolution kinetics of these minerals. The water column in the Weddell Gyre is oversaturated with respect to barite in the upper 1500 m with barely any regional variability (Fig. 6). This indicates that no dissolution of $BaSO_4$ should occur in the upper 1500 m of the water column. Based on the saturation state, no large Ba_d depth gradients are expected. Silicate shows a much larger surface to depth gradient since the entire oceanic water column is undersaturated ~~for~~ opal (Brzezinski et al., 2003; Hurd, 1972).

Regression of Ba_d against silicate shows a high correlation for the combined Prime Meridian and Weddell sections ($r^2 = 0.81$; Fig 7). The Ba_d-silicate regression for the Weddell region is slightly different from that for a meridional section south of the Polar Front along 30°E (1993 CIVA-1 cruise; WOCE I6 line, F. Dehairs & C. Jeandel, also in Fig. 7). For a given silicate concentration the Ba_d concentrations in the Weddell system exceed those at 30°E by about 5 nmol kg^{-1} - note that the 30°E section is quite near the far eastern rim of the Weddell Gyre. Also, the slope of the Ba_d versus silicate regression is larger ~~and~~ Ba_d intercept at zero silicate smaller ~~at 30°E~~ (differences are significant; $p<0.005$). In the Weddell region the higher Ba_d level highlights the decoupling between barium and silicate and points to a mechanism retaining Ba_d within the Gyre system relative to silicate. A likely mechanism is Ba translocation to particles in surface waters and ~~the~~ Ba efflux from the sediments as discussed below. However, a smaller biological ~~Ba over Si uptake ratio~~ in the upper waters of the Weddell Sea, as compared to the ACC could also lead to the peculiar Ba vs. silicate regression in the Weddell Gyre.

Barium depletion in the surface layer

~~Depletions of nutrients or~~ ~~TCO_2~~ in the surface layer ~~have~~ been used frequently to determine the net community production from the onset of the growth season until the time of measurement (e.g., Hoppema et al., 2007). We are using an approximate depletion here to obtain the seasonal changes of the Ba_d concentration between the winter and the time of sampling. Usually, depletions are computed from the vertical integration of ~~the substrate~~ concentration above the remnant Winter Water, which is identified by its temperature minimum, and is assumed to reflect the initial pre-bloom conditions. Since sampling resolution in the upper layers was insufficient to warrant a reliable integration over the surface layer, we simply consider the difference in Ba_d between the temperature minimum layer and

the shallowest sample (at about 20 m). This difference in Ba_d concentrations is proportional to the depletion and is an approximate measure of it.

At the Prime Meridian, the Ba_d difference between the temperature minimum and surface waters is generally in the range 0-6 nmol kg^{-1}, on average 3.6 ± 3.9 nmol kg^{-1} (Fig. 8A). A slight trend of higher values towards the centre of the transect may be discerned. At the Weddell section the Ba_d difference exhibits a range of -2 to 6 nmol kg^{-1}, with few deviations to higher and lower values (Fig. 8B). We further show that the Ba difference is independent on the temperature in the temperature minimum (Figs. 8C and 8D). At the Weddell section the temperature minimum remains close to the freezing point of seawater of -1.85°C and therefore it appears that the observed Ba_d depletions are real and not affected by erosion of the temperature minimum layer.

As a bio-intermediate element, Ba becomes depleted in the surface layer with respect to the deep water underneath it (e.g., Chan et al., 1977; Jacquet et al. 2007a). Our data show that surface water Ba depletions reaching up to 8 and 12 nmol kg^{-1} (for the Prime Meridian and Weddell section, respectively; Fig. 8) are generated within a few months since the end of winter. There are several possible processes that may be responsible for this: First, active or passive biologically-mediated uptake of Ba; and second, abiotic precipitation of Ba as the mineral barite ($BaSO_4$). As to the first cause, there are only very few phytoplankton species known to actively take up Ba (e.g., Gayral and Fresnel, 1979), which classifies active uptake rather as an unlikely contributor to Ba depletion. However, high particulate Ba concentrations have been reported in Southern Ocean surface waters (Cardinal et al., 2005; Jacquet et al., 2007a) usually associated with elevated biomass contents. This Ba is generally not present as barite (Dehairs et al., 1980; Stroobants et al., 1991), but is likely adsorbed onto organic matter (diatom tests; see Sternberg et al., 2005) or is incorporated into the skeletal matrix, e.g., in Acantharia (Bernstein et al., 1998; Jacquet et al., 2007b). As to the second cause, our results for Weddell Gyre surface waters point to a slight barite supersaturation in the upper water column with a maximum saturation index of 1.4 (Fig. 6). Monnin et al. (1999) and Monnin and Cividini (2006) identified the Weddell Sea as the only system in the world's ocean where $BaSO_4$ supersaturation prevails. Note that when barite saturation is reached, equilibrium should be the rule as expected for salts whose kinetics of dissolution/precipitation are generally believed to be fast. Nevertheless, large $BaSO_4$ supersaturations have also been documented for the sedimentary environment (e.g., Aloisi et al., 2004).

In the seasonally ice-covered Weddell Gyre a third cause of depletion should be considered, namely, barite precipitation during sea-ice formation. During ice formation in an already oversaturated surface ocean the salinity and solutes concentrations in brine channels may reach very high values (e.g., Anderson and Jones, 1985), eventually leading to extreme supersaturation of barite. This will result in inorganic precipitation of barite. The large biomass of sea-ice algae visible as green or brown ice at the base of ice floes may further enhance Ba depletion as a result of Ba adsorption on algal cells (thereby depleting also the surface water underneath the ice) and may also result in barite formation due to organic matter degradation within the sea-ice (Carson, 2008). Very high particulate Ba concentrations were measured in brown ice (up to 8 nM Ba correlating with high POC contents (EPOS-2 cruise; F. Dehairs unpublished results). Also, Carson (2008) reports dissolved Ba concentrations in sea-ice brine ranging widely from surface water values to as low as 6 nM. These observations suggest that significant Ba translocation from the dissolved to the particulate phase does occur in sea-ice brines. It is worthwhile contemplating that barite precipitation during sea-ice formation occurs in autumn and winter and therefore this process as such cannot explain the observed Ba_d depletion of the seasonal summer mixed-layer. However, barite formed within the sea ice will eventually be released in the surface waters, either during draining and flushing of brine waters or ultimately when the ice is melted at the end of the winter. The released barite cannot dissolve in the supersaturated surface waters but when associated with aggregates of ice algae it may sink out to the undersaturated deep ocean where it may eventually dissolve. Overall such a process would subtract Ba_d from surface waters and redistribute it in the deep ocean. As to the seasonal depletion, the melting of sea ice at the end of the winter will dilute the upper part of the winter mixed layer more than the lower part, which also has impact on the Ba_d concentrations. It also is manifest that the mechanism described above would lead to variability of the Ba_d depletion. Due to ice motion (which is different from the movement of the underlying water) and spatially variable rates of ice formation, the variation of Ba_d depletion is further enhanced and even enrichment (i.e. negative depletion; see Fig. 8B) of Ba_d is possible. We speculate that barite dissolution may even occur within the melting ice matrix in micro-environments with very low salinity, since the solubility of barite is higher at low salinity.

Ba_d concentrations in the surface waters are generally lower in the coastal current at the Prime Meridian (Fig. 3A), off Kapp Norvegia and off Joinville Island (Fig. 3B), than elsewhere in

the Weddell Gyre. There are two possible explanations for this, and one is related to sea-ice formation. Close to the coast, ice is formed ~~which is~~ blown off the coast by strong, cold winds; new ice is readily formed in the near coastal area ~~and therefore~~ these regions are sometimes denoted as sea-ice factories (e.g., Barber and Massom, 2007). ~~Hence, if~~ ice plays a major role in the depletion of Ba_d in the surface water, one would expect the lowest Ba_d concentrations near the coast ~~indeed~~. Another factor could be differences in upwelling rates, combined with biologically-mediated ~~draw-down~~ of Ba_d in the surface layer: ~~The~~ region with higher upwelling rates (bringing much Ba_d into the surface layer) would have ~~the~~ higher Ba_d concentration. Since upwelling in the divergent Weddell Gyre tends to occur towards its ~~centre~~, the coastal region ~~would~~ have lower Ba_d concentrations. This trend is reinforced by the higher biological activity at the shelves (Arrigo et al., 1998; Hoppema et al., 2007).

It is interesting to note that the larger surface Ba depletion around 62°S on the Prime Meridian (Fig. 8A) appears to coincide with elevated Ba_d concentrations in the deep basin between 2000 m and the bottom (Fig. 3A). This strongly hints at a mechanism whereby barite is being formed in the surface layer and is subsequently transferred to the deep ocean. At greater depths where undersaturation prevails (Fig. 6), dissolution of barite causes elevated concentrations of Ba_d. It should be added that this mechanism is not only active in the central Weddell Gyre; it is merely most ~~salient~~ there. ~~Also in~~ other parts of the basin the Ba_d concentration is to some degree determined by dissolution of barite – if the surface depletion of Ba_d is less, also less barite can be dissolved at depth. ~~Also note~~ that the vertical correspondence between Ba depletion in the surface and Ba enrichment at depth is not perfect because water currents (strength and direction) are depth-dependent. ~~That there is a good correspondence in the central gyre makes sense~~ because the currents are weakest there (Fahrbach et al., 1994).

Bottom layer enrichment

A remarkable observation is that both silicate and Ba_d are enriched in the bottom layer of the Weddell Sea; actually, the highest absolute concentrations of both species were observed there (Figs. 3B and 4B). For silicate this has been ~~reported early~~ by Edmond et al. (1979). Note, in contrast, that newly formed WSBW (which is the source of all bottom water in the Weddell Gyre) along the slope of the Antarctic Peninsula (Figs. 3B and 4B) is characterized by minima of silicate and Ba_d. This highlights that subsequent enrichment of bottom water occurs locally in the Weddell-Enderby basin. Even the spatial distributions of bottom layer

enrichment of silicate and dissolved Ba largely ~~conform;~~ Strong enrichments were found along most of the Weddell section (Figs. 3B and 4B), and at the Prime Meridian especially in the southern part (66.5-68.5°S; Fig. 3A and 4A). ~~Note, though, that in~~ the ~~north~~ of the Prime Meridian section at 55.5-56.5°S a silicate maximum was observed at the bottom, but this appears to be ~~spatially associated with deep waters;~~ no Ba_d analogue was found at that location. Hoppema et al. (1998) have demonstrated that ~~especially in the region off Kapp Norvegia~~ strong enrichment of the bottom water with silicate occurs, supported by a local bottom water recirculation cell. This could also explain higher Ba_d enrichment in that region.

Enrichment of Ba_d in the bottom layer may have two causes. First, particulate barite could ~~massively~~ dissolve at these depths because of the pressure dependence of the solubility product of barite (Monnin et al., 1999; Monnin and Cividini, 2006). ~~Note that the~~ saturation index Ω for $BaSO_4$ close to the seafloor at depths ~~>~~ 4000 m drops to values ~~as low as~~ < 0.6 (Fig. 6) and enhanced dissolution of barite may only ~~start at Ω well below 1,~~ due to kinetic effects. However, this explanation is unlikely since we found evidence for Ba_d enrichment in the deep water column (see above) which hints at dissolution at depths well above the bottom layer. Second, there may be input of Ba_d from the sediments to the overlying water. Biogenic barium is abundantly present in sediment cores from the Weddell Sea and environs (e.g., Ó Cofaigh and Dowdeswell, 2001). The occurrence of enhanced vertical gradients of Ba_d in the deepest samples combined with the fact that significant epibenthic flux of dissolved Ba to the water column has been reported for other oceanic areas as well (e.g., McManus et al., 1994, 1998), suggest that ~~efflux of Ba~~ from the sediments contributes to ~~the~~ elevated bottom water Ba concentrations. It is worthwhile adding that the spatial coincidence of Ba_d and silicate enrichment lends high credibility to the case for Ba_d input from the sediments because opal dissolution occurs ~~all through~~ the water column, and silicate effluxes from the sediments have been reported in the Weddell basin ~~indeed~~ (Edmond et al., 1979; Holby and Anderson, 1996; Rutgers van der Loeff and Van Bennekom, 1989).

A ~~very~~ rough estimation of the Ba flux from the sediments is presented. We take the Ba_d enrichment in the bottom layer to be 5 nmol kg^{-1}, where~~as~~ the vertical extent of that layer is about 500 m (~~see~~ Fig. 3B). This results in an enrichment of 2500 µmol m^{-2}. It has been generated at the time scale of the residence time of the WSBW in the bottom layer. The residence time is tentatively computed as 6 years, using the ~~horizontal extent~~ of the Weddell Gyre where WSBW occurs (assumed about $1 \cdot 10^{12}$ m^2), combined with the vertical extent (500

m) and the ventilation rate of WSBW (2.6 Sv = 2.6 10^6 m^3 s^{-1}; Fahrbach et al., 1994). This yields an efflux of Ba_d amounting to about 400 µmol m^{-2} yr^{-1}. This value falls well within the range reported in the literature for other open ocean environments, e.g., in the Equatorial Pacific: 160-1060 µmol m^{-2} yr^{-1} (McManus et al., 1999; Paytan and Kastner, 1996). Integrated over the Weddell Basin surface area of 1 10^{12} m^2 this adds up to 0.4 10^9 mol yr^{-1}.

Enrichment of dissolved barium in deep water

Since water mass transformation and mixing take place in the Weddell-Enderby basin, the bottom water Ba_d enrichment is also transferred to other water masses, in particular the voluminous deep water. We can make a rough estimation of the enrichment of Ba_d in the deep Weddell basin in the following way, using specific characteristics of the hydrography of the region. The main source of deep water of the Weddell Gyre is the inflowing CDW of the ACC near the eastern boundary. Other water masses are eventually derived from that source. At the Prime Meridian the source water mass can be distinguished at depths of about 200-1500 m at 64-69°S (see Fig. 2, and Hoppema et al., 1997). Its upper boundary is the θ maximum, while the lower boundary is distinguishable as a weak maximum both of TCO_2 and nutrients occurring at θ of about 0-0.2°C (Hoppema et al., 1997). We compare the Ba_d concentration of the CDW source water (marked as "inflow") with that of the remaining deep water masses at the Prime Meridian in a diagram of Ba_d against θ (Fig. 9). The Ba_d concentration in the inflow CDW tends to be lower than that in the rest of the basin - recall that lower Ba_d concentrations were observed in the CDW of the Antarctic Circumpolar Current indeed; see Results section and Fig. 3A. However, there is a large overlap of Ba_d values for the two sub-regions. At the highest θ values, representing the core of the θ maximum which is associated with inflowing CDW, Ba_d is the lowest (85-94 nmol kg^{-1}). Beneath the θ maximum of the inflow water, Ba_d is higher and similar to Ba_d in the low θ maximum of the remaining basin. In the deep Weddell basin with a θ range of roughly 0.2 to -0.7°C the Ba_d concentration is constant within about 93-101 nmol kg^{-1}. Some higher values of Ba_d appear to show enrichment in the bottom layer possibly resulting from epibenthic outflow of Ba (see above).

Since Ba_d in the water of about 0.5°C in the central and northern Weddell along the Prime meridian coincides with that of 0.5°C in the inflow area (64-69°S), it appears that the upper portion of the inflow water with the high θ maximum (>0.5°C) is upwelled into the surface layer during its further course through the gyre. Of note is that at the Prime Meridian we do

not catch the ~~whole~~ extent of upwelling of low-Ba_d subsurface water in the inflow. Actually, much upwelling has already taken place in the eastern Weddell Gyre between the eastern boundary and 0°E, changing water properties considerably (Bakker et al., 2008; Gouretski and Danilov, 1993). In the deep Weddell basin (θ about 0.2 to -0.7°C) the Ba_d concentration is higher than in the θ maximum layer but it is largely independent of θ (with a range of about 5 nmol kg^{-1}; Fig. 9). Further Ba_d enrichment occurs in the bottom layer (see above). This suggests that the Ba_d level of the deep water is fed by input from above (surface water) and below (water with θ<-0.7°C): Within the deep basin mixing and ~~uplifting~~ of ~~the~~ deep water takes place, which ~~relocates dissolved Ba~~. Another source of Ba_d ~~for~~ the deep Weddell Gyre is ~~the~~ dissolution of barite raining down from the upper layers, as the deep water below about 1500 m is undersaturated with respect to barite (Fig. 6).

Mass balance of Ba in the deep Weddell Gyre

We construct a tentative mass balance of Ba_d in the deep Weddell Gyre that must be consistent with the apparent enrichment of Ba_d within the Gyre compared to the source waters from the ACC. Orsi et al. (1999) estimated the total Antarctic Bottom Water export of the Atlantic sector of the Southern Ocean to be about 11Sv. This is too high for the Weddell Gyre because ~~Orsi et al.´s~~ definition of the Atlantic sector includes large regions east of the gyre. A value of 8-9 Sv may be more representative ~~for~~ the subsurface Weddell Gyre as reported by Klatt et al. (2005), although ~~also~~ this should be considered as upper boundary. This outflow must be balanced by an inflow of CDW and surface water from the ACC. The Ba concentration difference between the inflowing CDW with low Ba and outflowing deep water with high Ba amounts to about 5 nmol kg^{-1} (~~see~~ Fig. 9). Thus the net Ba loss of the Weddell Gyre to the ACC is about 40-45 mol s^{-1}, or 1.3-1.4·10^9 mol yr^{-1}. The deep Weddell Gyre also loses water and Ba_d to the surface layer through upwelling and diffusion. Different estimates are being reported for the rate of vertical advection in the Weddell Sea: Hoppema et al. (2001) give a lower end range between 0.5 and 1.3 Sv, while Weppernig et al. (1996), Mensch et al. (1996) and Haine et al. (1998) estimate vertical advection to range between 1.5 and 1.7 Sv. Taking a mean deep ocean to Winter Water ~~concentration~~ difference ~~of~~ ~~Ba_d~~ of 15 nmol kg^{-1}, vertical advection would convey between 0.6 - 0.8·10^9 mol ~~Ba_d~~ yr^{-1} from the deep water to the surface. The total loss from the deep Weddell Gyre thus amounts to 1.9-2.2·10^9 mol ~~Ba_d~~ yr^{-1}. Assuming steady state, this number must be identical to the supply of Ba_d to the deep water. The efflux of Ba from the Weddell Sea sediments contributes 0.4·10^9 mol yr^{-1} to the deep water (see above). We assume that the remaining 1.5-1.8·10^9 mol ~~Ba_d~~ yr^{-1} is ~~then by~~

difference contributed by supply from the surface layer, where Ba_d is subtracted and precipitated and brought to the deep Weddell as particulate matter, where it dissolves in the undersaturated ocean (see Fig. 6).

We calculated a net loss of Ba_d of the Weddell Gyre, but it should be stressed that this is only a loss from the *deep* gyre. This excess Ba_d originates predominantly from the surface layer. The surface layer of the Weddell Gyre is eventually generated through upwelling of CDW. It is manifest that the Ba_d concentration in the surface layer is much lower than that of the CDW, evidencing that Ba_d is lost from the surface layer. This loss is affected by biologically-mediated processes of Ba subtraction and barite formation within the sea ice (see above). The Ba depleted surface water is transferred equatorwards from the Weddell Gyre through Ekman transport.

Considering a Weddell surface area of $1 \cdot 10^{12}$ m^2, the Ba_d supply needed for making up the balance for the deep Weddell Gyre equals 4-5 µmol m^{-2} d^{-1}. This is similar but generally somewhat larger than the Ba fluxes recorded by deep water sediment traps elsewhere. A trap at 4023 m from site M2 (French KERFIX/ANTARES program 1994-1995) located in the ACC beyond the eastern rim of the Weddell Gyre in the Indian sector (52°S – 61°32'E) recorded Ba fluxes between 0.2 and 2.8 µmol m^{-2} d^{-1} (average flux = 0.94 µmol m^{-2} d^{-1}; Jeandel et al., unpublished results). At the M3 site (63°S-71°E; KERFIX/ANTARES program) in the SIZ further south, Ba fluxes at 1334 m and 3444 m were smaller (range: 0.06 to 0.34 µmol m^{-2} d^{-1}; average = 0.14 µmol m^{-2} d^{-1} and range 0.09 to 0.38 µmol m^{-2} d^{-1}; average = 0.22 µmol m^{-2} d^{-1}, respectively; Jeandel et al., unpublished results). Sediment traps moored in the Polar Frontal Zone, along 145°E, had average Ba fluxes of 0.74 and 0.68 µmol m^{-2} d^{-1} at 800 and 1580 m, respectively (Jacquet et al., 2007a). The particulate Ba subtraction estimated here also is similar to the seasonal input of particulate Ba in the mesopelagic waters (as a result of barite precipitation in decomposing sinking aggregates) of the Polar Front along 6°W (1.4 µmol m^{-2} d^{-1}; Dehairs et al., 1997) which represents at least part of the vertical flux of Ba in the water column. The derived apparent fluxes in the deep Weddell Gyre are likely to be on the high side. On the other hand, the total enrichment of Ba_d must by nature be larger than the particulate Ba fluxes captured by traps because the material caught in the traps is only part of the total, the rest having been dissolved on the way. Finally, subtraction of Ba in the surface layer from solution via barite precipitation associated with sea-ice formation and

biological activity may be more efficient in the Weddell Gyre than in other regions because of the large sea ice formation in the ~~latter region~~.

Concluding remarks

Two full-depth sections have provided insight into the factors determining the Ba_d distribution. The Weddell Gyre is supplied with deep water from the ACC, which is relatively low in Ba_d. The low Ba_d concentration could still be observed at the Prime Meridian (which is some distance away from the actual ACC source). In the gyre this low-Ba_d subsurface water is upwelled into the surface layer. Further decrease of Ba_d in the surface layer occurs due to Ba uptake as a consequence of phytoplankton activity, complemented by barite formation in sea-ice. Within the voluminous deep Weddell Gyre, Ba_d is enriched compared to the source water of the gyre. This is ~~effectuated~~ by two processes; first, barite dissolution in the undersaturated deep water, with barite originating from the depleted surface layer; and second by Ba_d mixing into the deep water from the strongly Ba_d enriched bottom layer. Ba_d influx from the bottom layer seems to occur predominantly in the southeastern part of the Weddell basin, in exactly the same region where bottom layer enrichment of silicate occurs. Water movement and circulation further redistribute Ba_d through the Weddell-Enderby basin. Tentative calculations ~~showed~~ that enrichment of the deep water due to Ba_d originating from the surface layer is likely to be larger than through Ba_d supply from the bottom layer. Locally this may ~~certainly~~ be variable.

Summarizing, a mechanism appears to exist ~~in which~~ the Weddell Gyre acts as an efficient conduit for Ba_d export to the deep and abyssal world oceans. In the surface layer Ba_d is ~~subtracted~~ due to phytoplankton activity and barite precipitation within sea ice. This particulate, absorbed and adsorbed Ba is subsequently exported from the surface layer by ~~gravitational action~~ and redissolves in the deep Weddell Gyre. The deep water, classified as Antarctic Bottom Water, thus enriched in Ba_d ~~abandons~~ the gyre to replenish the abyssal ocean basins to the north. Ba_d depleted surface water leaves the gyre northwards through Ekman transport.

Acknowledgements

This research was supported by the Federal Belgian Science Policy Office (Belspo) under the Science for Sustainable Development (SDD) programme, Brussels, Belgium (BELCANTO contract SD/CA/03A) and Vrije Universiteit Brussel (project GOA 53). We thank Evaline van

Weerlee (NIOZ, Texel) for the silicate measurements on board Polarstern and Rob Middag (NIOZ) for help with sampling for barium. We are grateful to the captain and crew of Polarstern for their hospitality and help. This work was partly funded by the EU IP CARBOOCEAN (project nr. 511176, GOCE).

References

Aloisi G, Wallmann K, Bollwerk SM, Derkachev A, Bohrmann G, Suess E. The effect of dissolved barium on biogeochemical processes at cold seeps, Geochim Cosmochim Acta 2004;68:1735-48.

Anderson LG, Jones EP. Measurements of total alkalinity, calcium, and sulfate in natural sea ice. J Geophys Res 1985;90:9194-8.

Arrigo KR, Worthen D, Schnell A, Lizotte MP. Primary production in Southern Ocean waters. J Geophys Res 1998;103:15587-600.

Bakker DCE, Hoppema M, Schröder M, Geibert W, De Baar HJW. A rapid transition from ice covered CO_2-rich waters to a biologically mediated CO_2 sink in the eastern Weddell Gyre. Biogeosciences 2008;5:1373-86.

Barber DG, Massom RA. The role of sea ice in Arctic and Antarctic polynyas. In: Smith Jr WO, Barber DG, editors. Polynyas: Windows to the world. Elsevier Oceanography Series 74. Amsterdam: Elsevier; 2007. p. 1-54.

Bernstein RE, Byrne RH, Schijf J. Acantharians: A missing link in the oceanic biogeochemistry of barium. Deep-Sea Res I 1998;45:491-505.

Bertram MA, Cowen JP. Morphological and compositional evidence for biotic precipitation of marine barite. J Mar Res 1997;55:577-93.

Brzezinski MA, Jones JL, Bidle KD, Azam F. The balance between silica production and silica dissolution in the sea: Insights from Monterey Bay, California, applied to the global data set. Limnol Oceanogr 2003;48:1846-54.

Cardinal D, Savoye N, Trull TW, André L, Kopczynska EE, Dehairs F. Variations of carbon remineralisation in the Southern Ocean illustrated by the Ba_{xs} proxy. Deep-Sea Res I 2005;52:355-70.

Carson DS. Biogeochemical controls on paleoceanographic proxies: The Antarctic sea ice environment. PhD Thesis. University of Edinburgh; 2008.

Chan LH, Drummond D, Edmond JM, Grant B. On the barium data from the Atlantic GEOSECS Expedition. Deep-Sea Res 1977;24:613-49.

Dehairs F, Chesselet R, Jedwab J. Discrete suspended particles of barite and the barium cycle in the open ocean. Earth Planet Sci Letters 1980;49:528-50.

Dehairs F, Goeyens L, Stroobants N, Bernard P, Goyet C, Poisson A, Chesselet R. On suspended barite and the oxygen minimum in the Southern Ocean. Global Biogeochem Cycles 1990;4:85-102.

Dehairs F, Shopova D, Ober S, Veth C, Goeyens L. Particulate barium stocks and oxygen consumption in the Southern Ocean mesopelagic water column during spring and early summer: Relationship with export production. Deep-Sea Res II 1997;44:497-516.

Dehairs F, Jacquet S, Savoye N, Van Mooy BAS, Buesseler KO, Bishop JKB, Lamborg CH, Elskens M, Baeyens W, Boyd PW, Casciotti KL, Monnin C. Barium in twilight zone suspended matter as a potential proxy for particulate organic carbon remineralization: Results for the North Pacific. Deep-Sea Res II 2008;55:1673-83.

Edmond JM, Jacobs SS, Gordon AL, Mantyla AW, Weiss RF. Water column anomalies in dissolved silica over opaline sediments and the origin of the deep silica maximum. J Geophys Res 1979;84:7809-26.

Fahrbach E (editor). The Expedition ANTARKTIS-XXII/3 of the research vessel "Polarstern" in 2005. Berichte zur Polar- und Meeresforschung 2006;533:1-246.

Fahrbach E, Rohardt G, Schröder M, Strass V. Transport and structure of the Weddell Gyre. Annales Geophysicae 1994;12:840-55.

Fahrbach E, Harms S, Rohardt G, Schröder M, Woodgate RA. Flow of bottom water in the northwestern Weddell Sea. J Geophys Res 2001;106:2761-78.

Fresnel J, Galle P, Gayral P. Résultats de la microanalyse des cristaux vacuaolaires chez deux Chromophytes unicellulaires marines: *Exanthemachrysis gayraliae*, Pavlova sp. (Prymnésiophycées, Pavlovacées), C. R. Acad Sci Paris 1979;288D:823-5.

Ganeshram RS, François R, Commeau J, Brown-Leger SL. An experimental investigation of barite formation in seawater. Geochim Cosmochim Acta 2003;67:2599-2605.

Gayral P, Fresnel J. *Exanthemachrysis gayraliae* lepailleur (Prymnesiophyceae, Pavlovales): Ultrastructure et discussion taxinomique. Protistologica 1979;15:271-82.

Gordon AL, Huber BA, Hellmer HH, Ffield A. Deep and bottom water of the Weddell Sea´s western rim. Science 1993;262:95-97.

Gouretski VV, Danilov AI. Weddell Gyre: Structure of the eastern boundary. Deep-Sea Res I 1993;40:561-82.

Haine TWN, Watson AJ, Liddicoat MI, Dickson RR. The flow of Antarctic Bottom Water to the southwest Indian Ocean estimated using CFCs. J Geophys Res 1998;103:27637-53.

Holby O, Anderson LG. Geochemistry in an area recently uncovered from the Filchner Ice Shelf. Continental Shelf Res 1996;16:1479-88.

Hoppema M, Fahrbach E, Schröder M. On the total carbon dioxide and oxygen signature of the Circumpolar Deep Water in the Weddell Gyre. Oceanol Acta 1997;20:783-798.

Hoppema M, Fahrbach E, Richter K-U, De Baar HJW, Kattner G. Enrichment of silicate and CO_2 and circulation of the bottom water in the Weddell Sea. Deep-Sea Res I 1998;45:1793-1813.

Hoppema M, Klatt O, Roether W, Fahrbach E, Bulsiewicz K, Rodehacke C, Rohardt G. Prominent renewal of Weddell Sea Deep Water from a remote source. J Mar Res 2001;59:257-279.

Hoppema M, Middag R, De Baar HJW, Fahrbach E, Van Weerlee EM, Thomas H. Whole season net community production in the Weddell Sea. Polar Biol 2007;31:101-111.

Hopwood JD, Mann S, Gooday AJ. The crystallography and possible origin of barium sulphate in deep sea Rhizopod protists (Xenophyophorea). J Mar Biol Assoc UK 1997;77:969-87.

Hurd DC. Factors affecting the solution rate of biogenic opal in seawater. Earth Planet Sci Letters 1972;15**:**411-7.

Jacquet SHM. Barium in the Southern Ocean: Towards an estimation of twilight zone C mineralization. Doctoral Thesis. Vrije Universiteit Brussel, 234 pp; 2007.

Jacquet SHM, Dehairs F, Cardinal D, Navez J, Delille B. Barium distribution across the Southern Ocean frontal system in the Crozet–Kerguelen Basin. Mar Chem 2005; 95;142-62.

Jacquet SHM, Dehairs F, Rintoul S. A high resolution transect of dissolved barium in the Southern Ocean. Geophys Res Letters 2004;31:L14301. doi:10.1029/2004GL020016.

Jacquet SHM, Dehairs F, Elskens M , Savoye N, Cardinal D. Barium cycling along WOCE SR3 line in the Southern Ocean. Mar Chem 2007a;106:33-45.

Jacquet SHM, Henjes J, Dehairs F, Worobiec A, Savoye N, Cardinal D. Particulate Ba-barite and acantharians in the Southern Ocean during the European Iron Fertilization Experiment (EIFEX). J Geophys Res 2007b;112:G04006. doi:10.1029/2006JG000394.

Jacquet SHM, Dehairs F, Savoye N, Obernosterer I, Christaki U, Monnin C, Cardinal D. Mesopelagic organic carbon remineralization in the Kerguelen Plateau region tracked by biogenic particulate Ba. Deep-Sea Res II 2008;55:868-79.

Jeandel C, Dupré B, Lebaron G, Monnin C, Minster J-F. Longitudinal distributions of dissolved barium, silica and alkalinity in the western and southern Indian Ocean. Deep-Sea Res I 1996;43:1-31.

Jochem FJ, Mathot S, Quéguiner B. Size-fractionated primary production in the open Southern Ocean in austral spring. Polar Biol 1995;15:381-92.

Klatt O, Fahrbach E, Hoppema M, Rohardt G. The transport of the Weddell Gyre across the Prime Meridian. Deep-Sea Res II 2005;52:513-528.

Klinkenberg H, Van Borm W, Souren F. A theoretical adaptation of the classical isotope dilution technique for practical routine analytical determinations by means of inductively coupled plasma mass spectrometry. Spectrochimica Acta Part B: Atomic Spectroscopy 1996;51:139-53.

McManus J, Berelson WM, Hammond DE, Klinkhammer GP. Barium cycling in the North Pacific: Implications for the utility of Ba as a paleoproductivity and paleoalkalinity proxy. Paleoceanography 1999;14:53-61.

McManus J, Berelson WM, Klinkhammer GP, Johnson KS, Coale KH, Anderson RF, Kumar N, Burdige DJ, Hammond DE, Brumsack HJ, McCorkle DC, Rushdi A. Geochemistry of barium in marine sediments: Implications for its use as a paleoproxy. Geochim Cosmochim Acta 1998;62:3453-73.

McManus J, Berelson WM, Klinkhammer GP, Kilgore TE, Hammond DE. Remobilization of barium in continental margin sediments. Geochim Cosmochim Acta 1994;58:4899-4907.

Mensch M, Bayer R, Bullister JL, Schlosser P, Weiss RF. The distribution of tritium and CFCs in the Weddell Sea during the mid-1980s. Progr Oceanogr 1996;38:377-415.

Meredith MP, Locarnini RA, Van Scoy KA, Watson AJ, Heywood KJ, King BA. On the sources of Weddell Gyre Antarctic Bottom Water. J Geophys Res 2000;105:1093-1104.

Monnin C. Density calculations and concentration scale conversions for natural waters. Computers and Geosciences 1994;20:1435-45.

Monnin C. A thermodynamic model for the solubility of barite and celestite in electrolyte solutions and seawater from 0 to 200°C and to 1 kbar. Chem Geol 1999;153:187–209.

Monnin C, Jeandel C, Cattaldo T, Dehairs F. The marine barite saturation state of the world's oceans. Mar Chem 1999;65:253-61.

Monnin C, Cividini D. The saturation state of the world's ocean with respect to $(Ba,Sr)SO_4$ solid solutions. Geochim Cosmochim Acta 2006;70:3290-8.

Moore JK, Abbott MR, Richmann G, Smith WO, Cowles JC, Coale KH, Gardner WD, Barber RT. SeaWiFS satellite ocean color data from the Southern Ocean, Geophys Res Letters 1999;26:1465-8.

Ó Cofaigh C, Dowdeswell JA. Late quaternary iceberg rafting along the Antarctic Peninsula continental rise and in the Weddell and Scotia Seas. Quarternary Res 2001;56:308-21.

Orsi AH, Nowlin Jr. WD, Whitworth III T. On the circulation and stratification of the Weddell Gyre. Deep-Sea Res I 1993;40:169-203.

Orsi AH, Johnson GC, Bullister JL. Circulation, mixing, and production of Antarctic Bottom Water. Progr Oceanogr 1999;43:55-109.

Paytan A, Kastner M. Benthic Ba fluxes in the central Equatorial Pacific, implications for the oceanic Ba cycle. Earth Planet Sci Letters 1996;142:439-50.

Rutgers van der Loeff MM, Van Bennekom AJ. Weddell Sea contributes little to silicate enrichment in Antarctic Bottom Water. Deep-Sea Res 1989;36:1341-57.

Savoye N, Dehairs F, Elskens M, Cardinal D, Kopczynska EE, Trull TW, Wright S, Baeyens W, Griffiths FB. Regional variation of spring N-uptake and new production in the Southern Ocean. Geophys Res Letters 2004;31:L03301,10.1029/2003GL018946.

Sternberg E, Tang D, Ho T-Y, Jeandel C, Morel FMM. Barium uptake and adsorption in diatoms. Geochim Cosmochim Acta 2005;69 :2745-52.

Stroobants N, Dehairs F, Goeyens L, Vanderheijden N, Van Grieken R. Barite formation in the Southern Ocean water column. Mar Chem 1991;35:411-21.

Webster RK. 1960. Mass Spectrometric Isotope Dilution Analysis. In: Smales AA, Wager LR, editors. Methods in Geochemistry. New York: Interscience; 1960. p. 202-46.

Weppernig R, Schlosser P, Khatiwala S, Fairbanks RG. Isotope data from Ice Station Weddell: Implications for deep water formation in the Weddell Sea. J Geophys Res 1996;101:25723-39.

Figure captions

Figure 1

Map of the Weddell Sea and environs with station locations during cruise ANT-XXII/3. Arrows denote the schematic surface circulation in the region.

Figure 2

Section at the Prime Meridian cutting the Weddell Gyre and the southernmost part of the Antarctic Circumpolar Current, contoured for potential temperature (°C) at cruise ANT-XXII/3 in 2005.

Figure 3

Sections contoured for dissolved barium (nmol kg^{-1}) during cruise ANT-XXII/3 in 2005, A) at the Prime Meridian cutting the Weddell Gyre and the southernmost part of the Antarctic Circumpolar Current; and B) across the Weddell Sea from Kapp Norvegia (right) to Joinville Island at the tip of the Antarctic Peninsula (left).

Figure 4

Sections contoured for dissolved silicate (μmol kg^{-1}) during cruise ANT-XXII/3 in 2005, A) at the Prime Meridian cutting the Weddell Gyre and the southernmost part of the Antarctic Circumpolar Current; and B) across the Weddell Sea from Kapp Norvegia (right) to Joinville Island at the tip of the Antarctic Peninsula (left).

Figure 5

Plots of silicate (µmol kg^{-1}) vs. salinity (A, B) and dissolved Ba (nmol kg^{-1}) vs. salinity (C, D) for the Weddell and the Prime Meridian sections to investigate property maxima in the deep water.

Figure 6

Barite saturation state Ω (ion product of Ba and sulfate divided by the solubility of barite) for the sections along the Prime Meridian (A) and across the Weddell Sea (B). If Ω >1 the water is supersaturated with barite.

Figure 7

Dissolved Ba (nmol kg^{-1}) plotted against silicate (µmol kg^{-1}) for data from the Prime Meridian and Weddell sections combined. Also shown is the regression for a section at 30°E (1993, CIVA1 cruise, WOCE I6 line) where only stations south of the Polar Front were included.

Figure 8

Dissolved barium concentration difference between the temperature minimum layer and the near-surface in the surface layer vs. latitude at the Prime Meridian (A), and vs. longitude at the Weddell section (B). The same Ba difference plotted against the potential temperature of the temperature minimum layer at the Prime Meridian (C) and at the Weddell section (D).

Figure 9

Dissolved barium plotted against potential temperature. Data are from the Prime Meridian section only; surface layer data are excluded.

Figure(s)

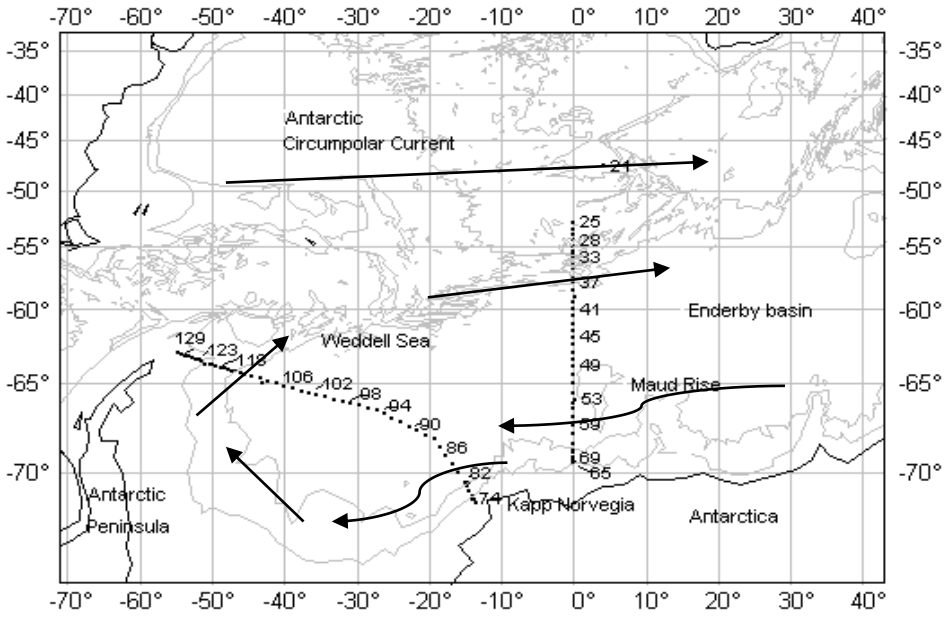

Source: GEBCO.

FIGURE 1

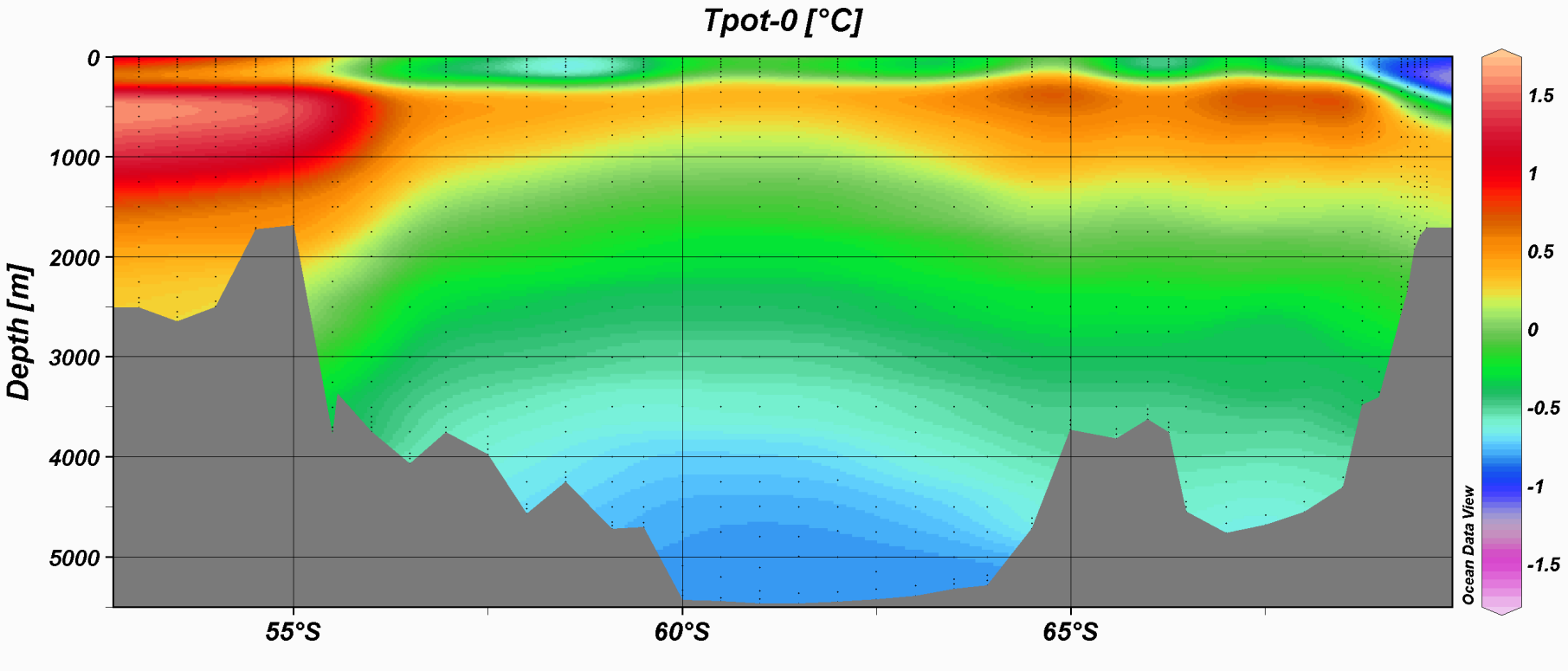
Tpot-0 [°C]
Depth [m]
0
1000
2000
3000
4000
5000
55°S
60°S
65°S
1.5
1
0.5
0
-0.5
-1
-1.5
Ocean Data View

FIGURE 2

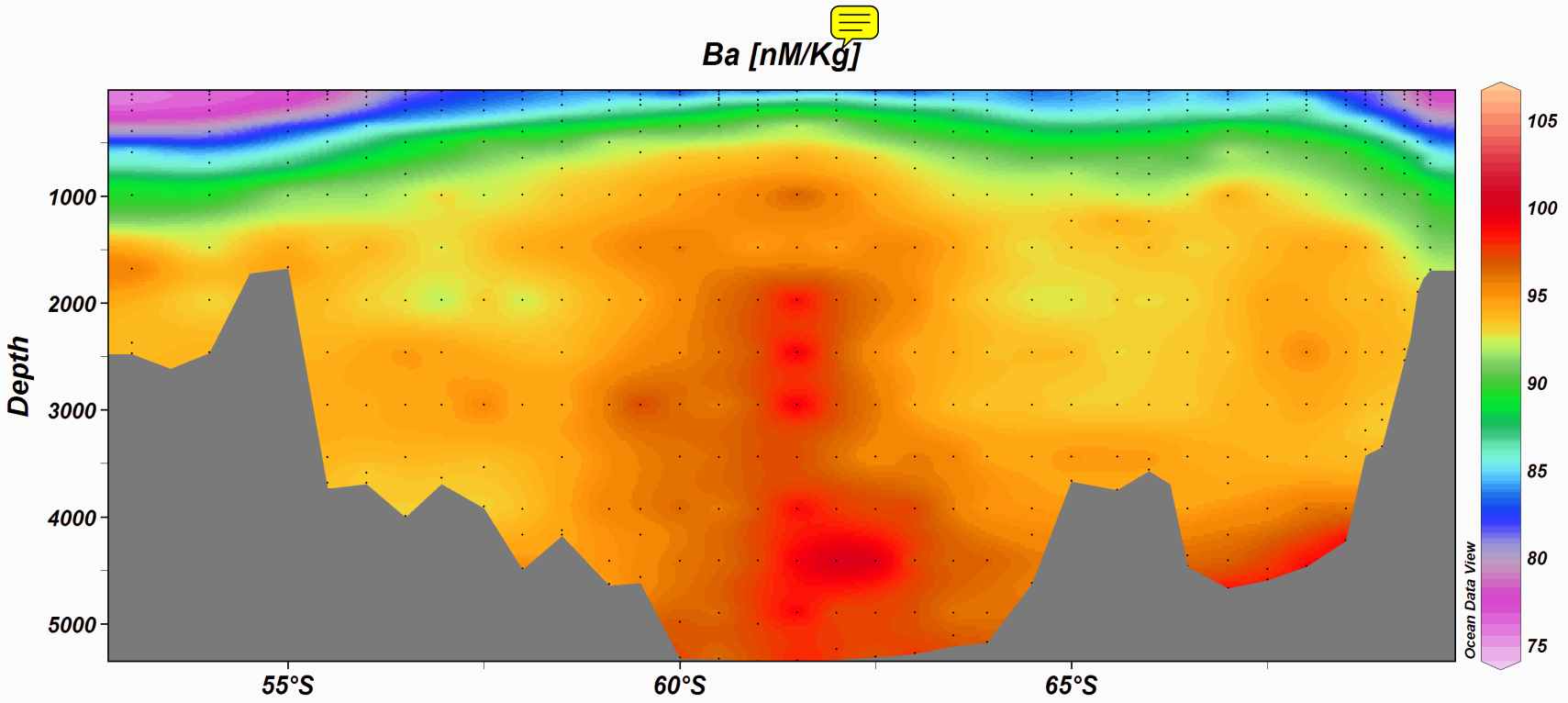
Ba [nM/Kg]
Depth
1000
2000
3000
4000
5000
55°S
60°S
65°S
105
100
95
90
85
80
75
Ocean Data View

FIGURE 3A

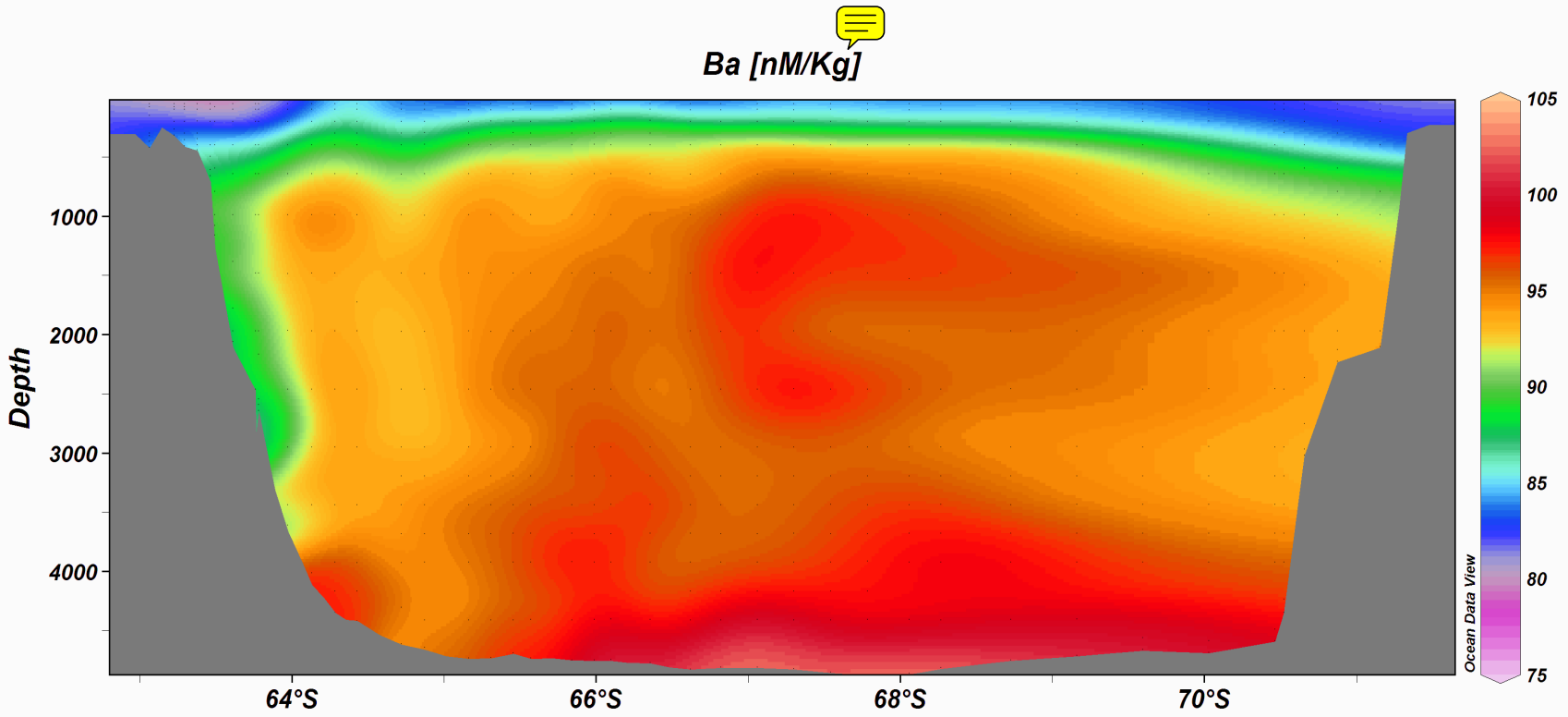
Ba [nM/Kg]
Depth
1000
2000
3000
4000
64°S
66°S
68°S
70°S
105
100
95
90
85
80
75
Ocean Data View

FIGURE 3B

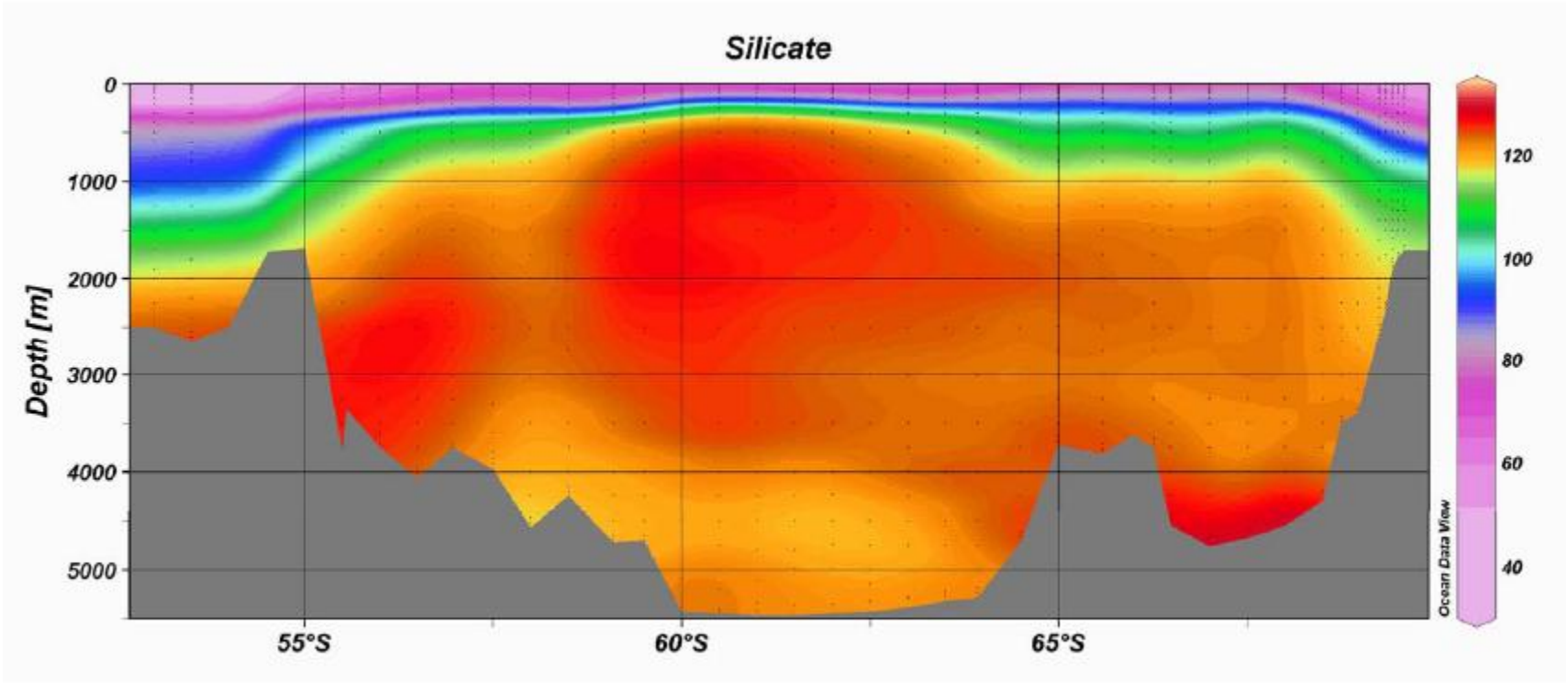
Silicate
Depth [m]
0
1000
2000
3000
4000
5000
55°S
60°S
65°S
120
100
80
60
40
Ocean Data View

FIGURE 4A

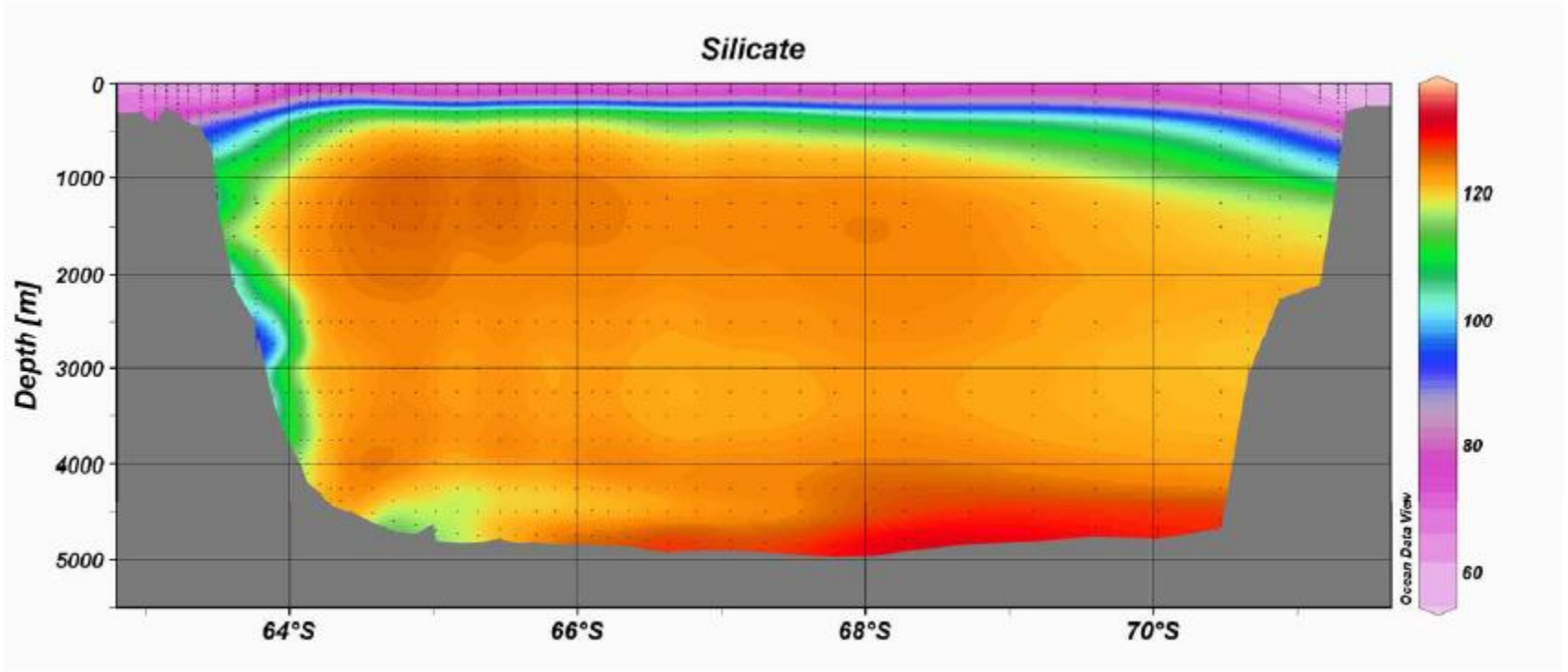
Silicate
0
1000
2000
3000
4000
5000
Depth [m]
64°S
66°S
68°S
70°S
120
100
80
60
Ocean Data View

FIGURE 4B

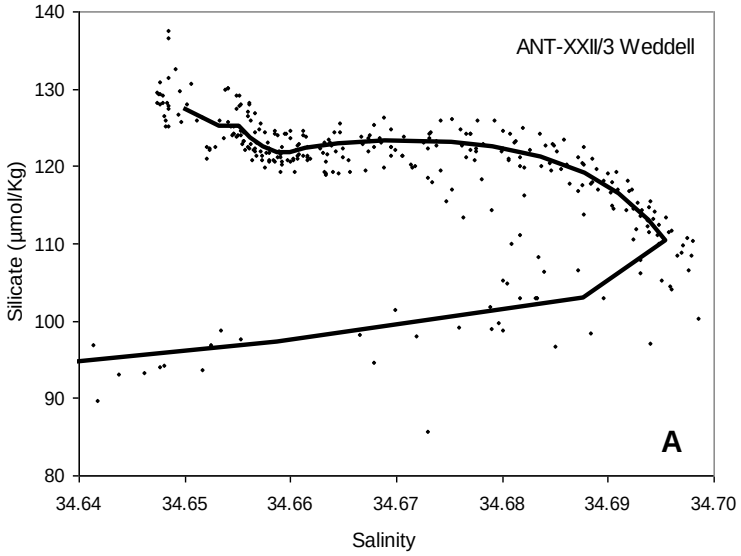
ANT-XXII/3 Weddell
Silicate (µmol/Kg)
Salinity
A

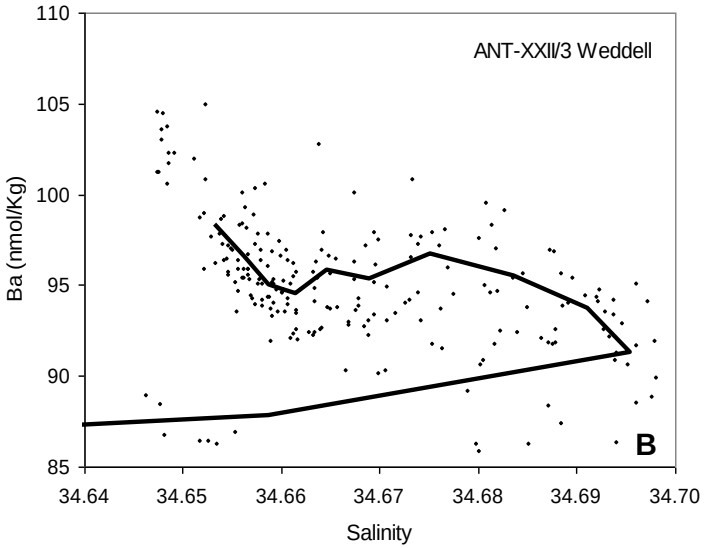
ANT-XXII/3 Weddell
Ba (nmol/Kg)
Salinity
B

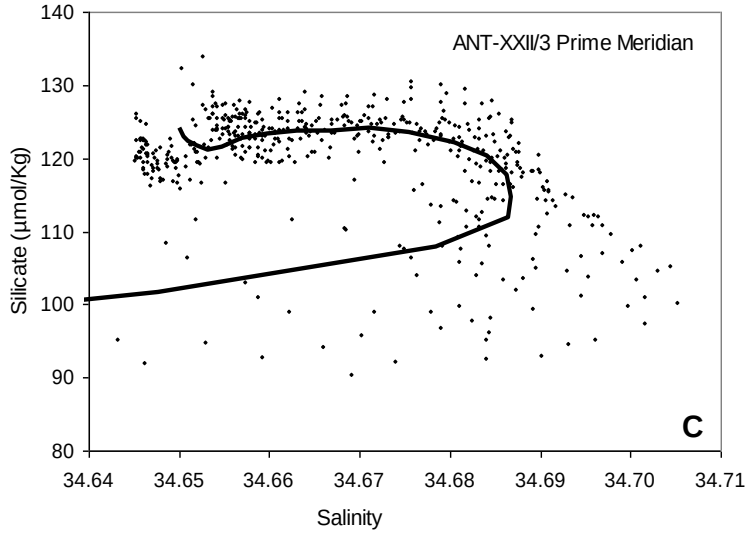
ANT-XXII/3 Prime Meridian
Silicate (µmol/Kg)
Salinity
C

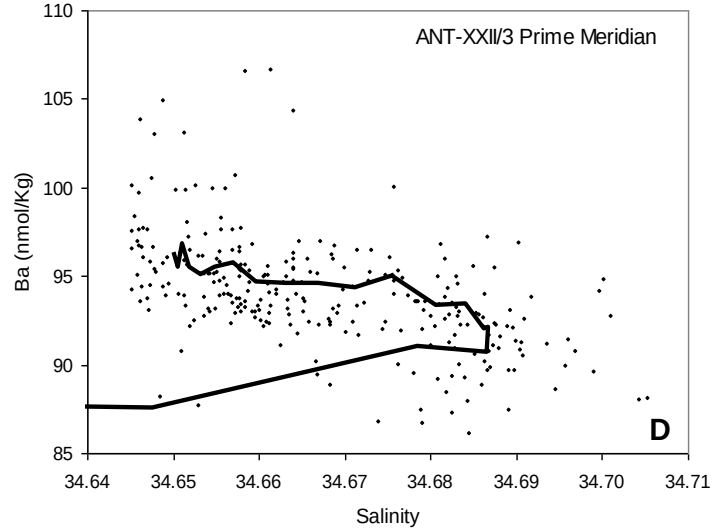
ANT-XXII/3 Prime Meridian
Ba (nmol/Kg)
Salinity
D

FIGURE 5

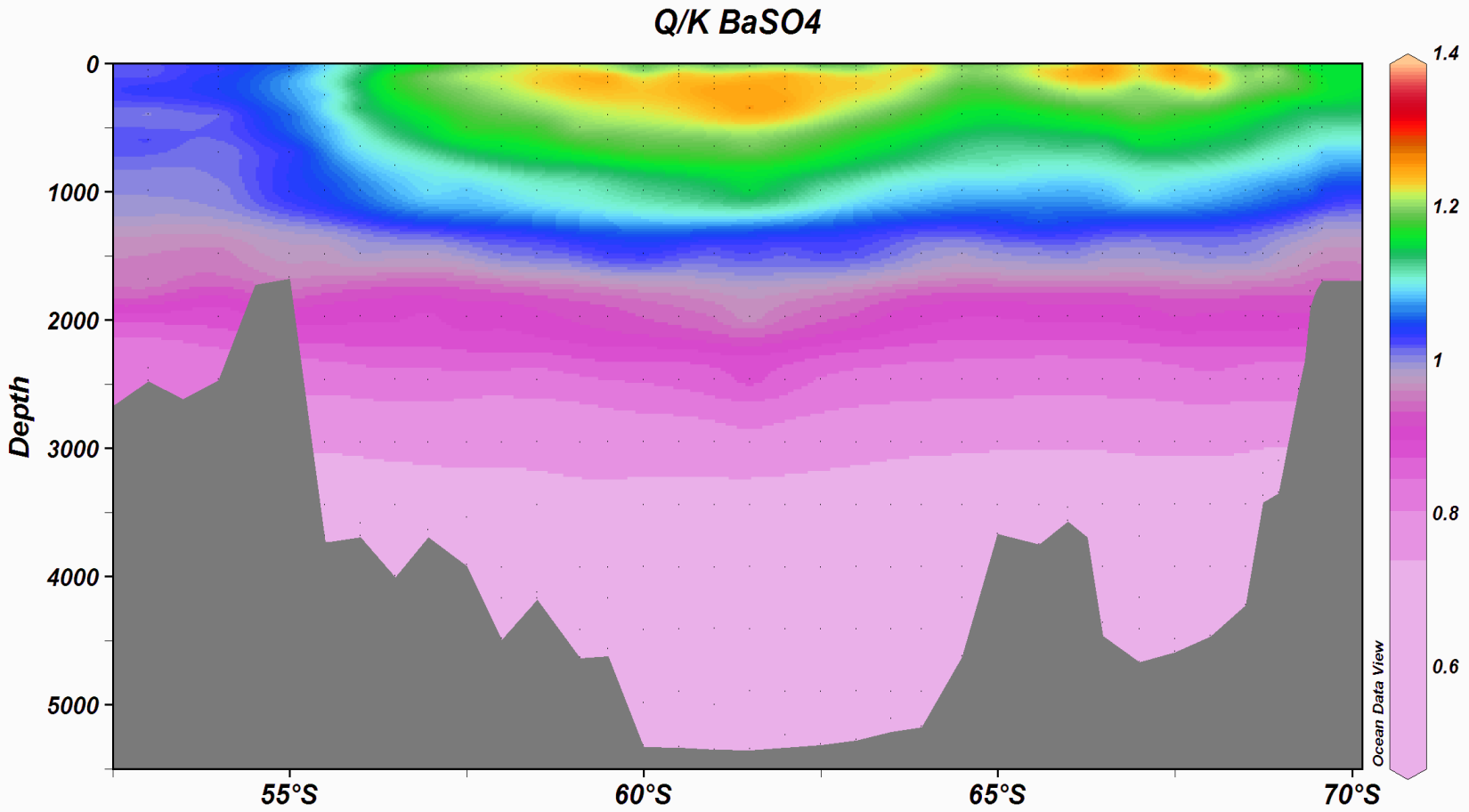
Q/K BaSO4
Depth
0
1000
2000
3000
4000
5000
55°S
60°S
65°S
70°S
1.4
1.2
1
0.8
0.6
Ocean Data View

FIGURE 6A

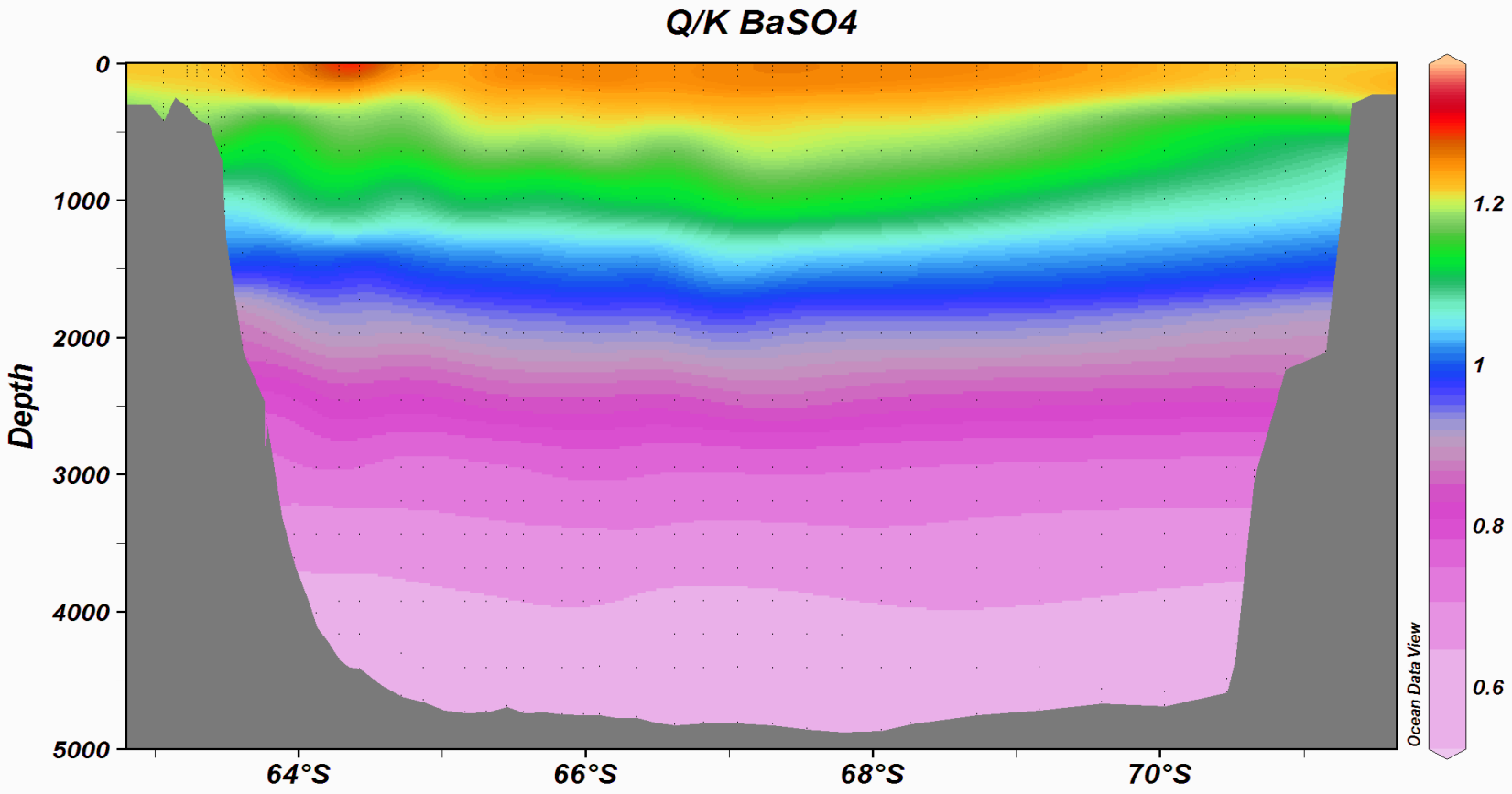
Q/K BaSO4
Depth
0
1000
2000
3000
4000
5000
64°S
66°S
68°S
70°S
1.2
1
0.8
0.6
Ocean Data View

FIGURE 6B

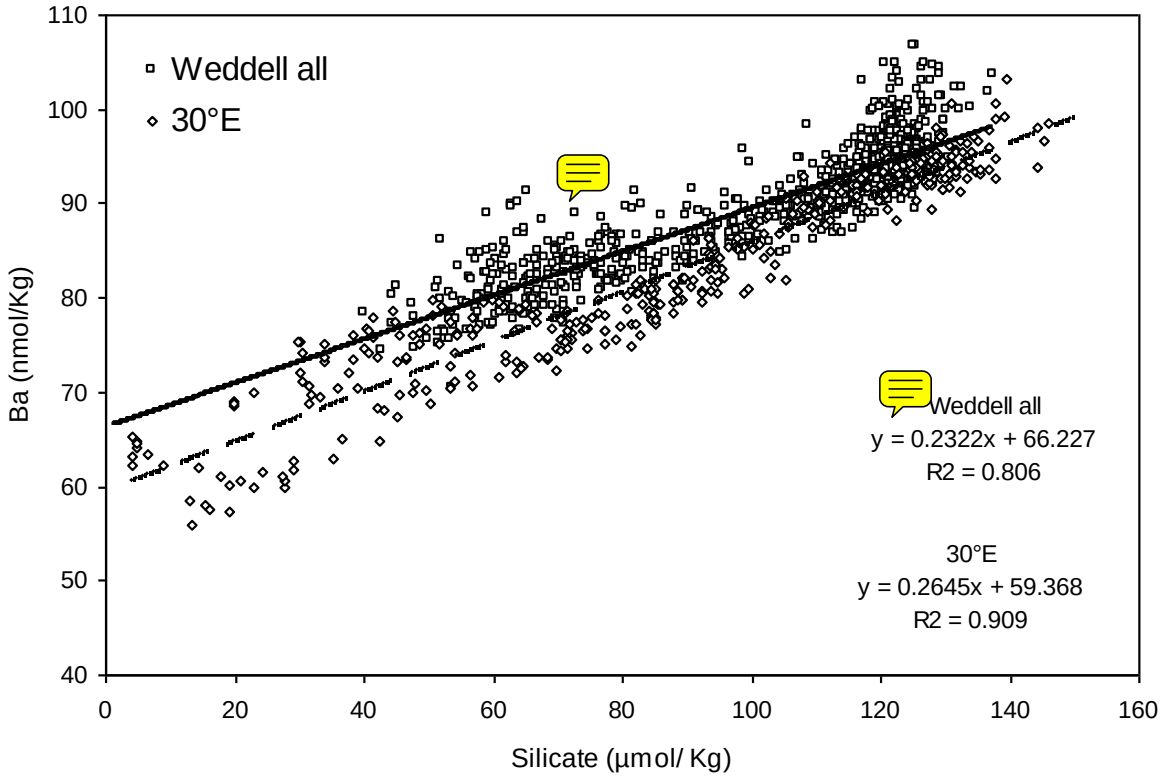
Weddell all
30°E
Ba (nmol/Kg)
Silicate (µmol/ Kg)
Weddell all
y = 0.2322x + 66.227
R2 = 0.806
30°E
y = 0.2645x + 59.368
R2 = 0.909
110
100
90
80
70
60
50
40
0
20
40
60
80
100
120
140
160

FIGURE 7

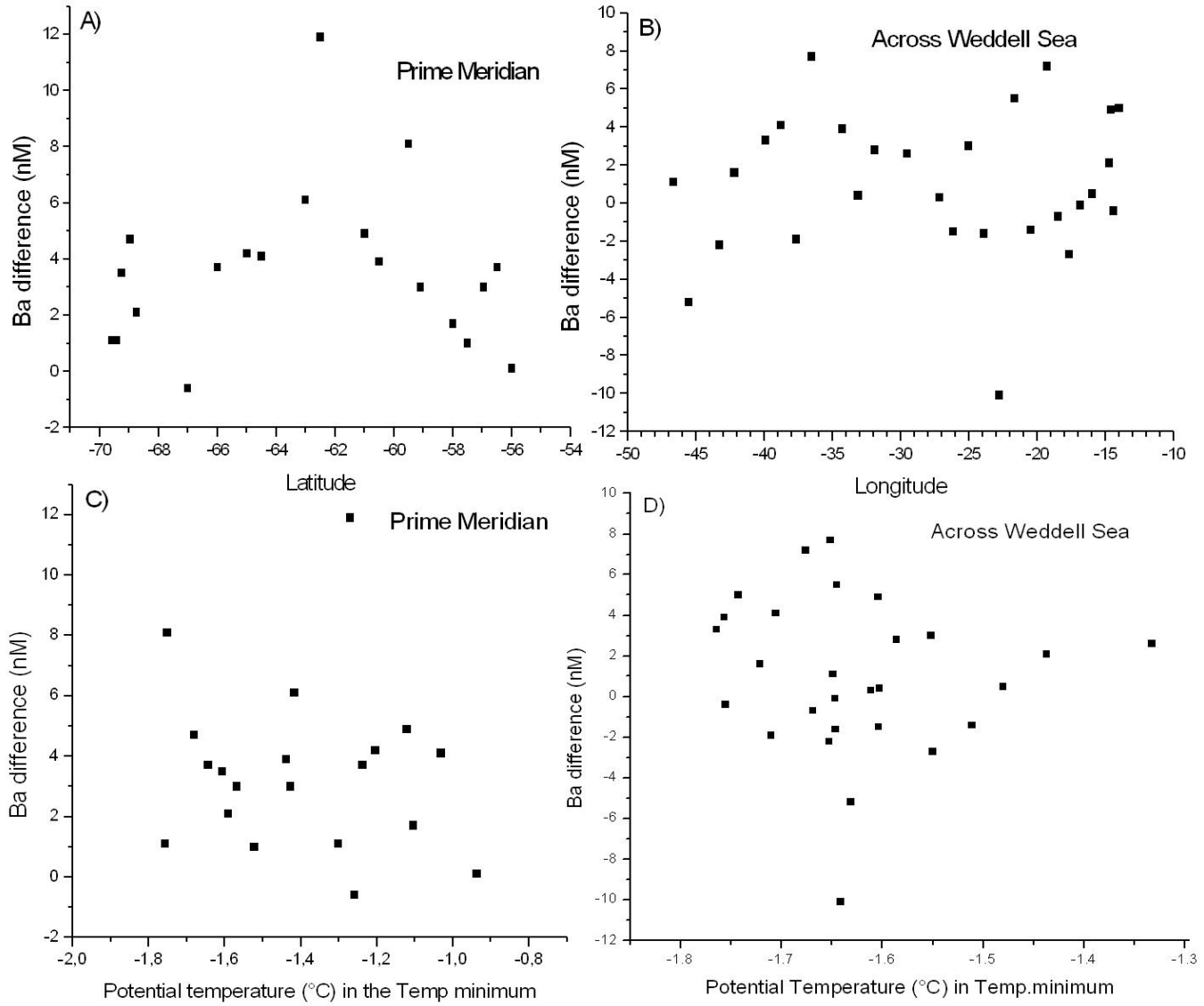
A)
Prime Meridian
Ba difference (nM)
Latitude
B)
Across Weddell Sea
Ba difference (nM)
Longitude
C)
Prime Meridian
Ba difference (nM)
Potential temperature (°C) in the Temp minimum
D)
Across Weddell Sea
Ba difference (nM)
Potential Temperature (°C) in Temp.minimum

FIGURE 8

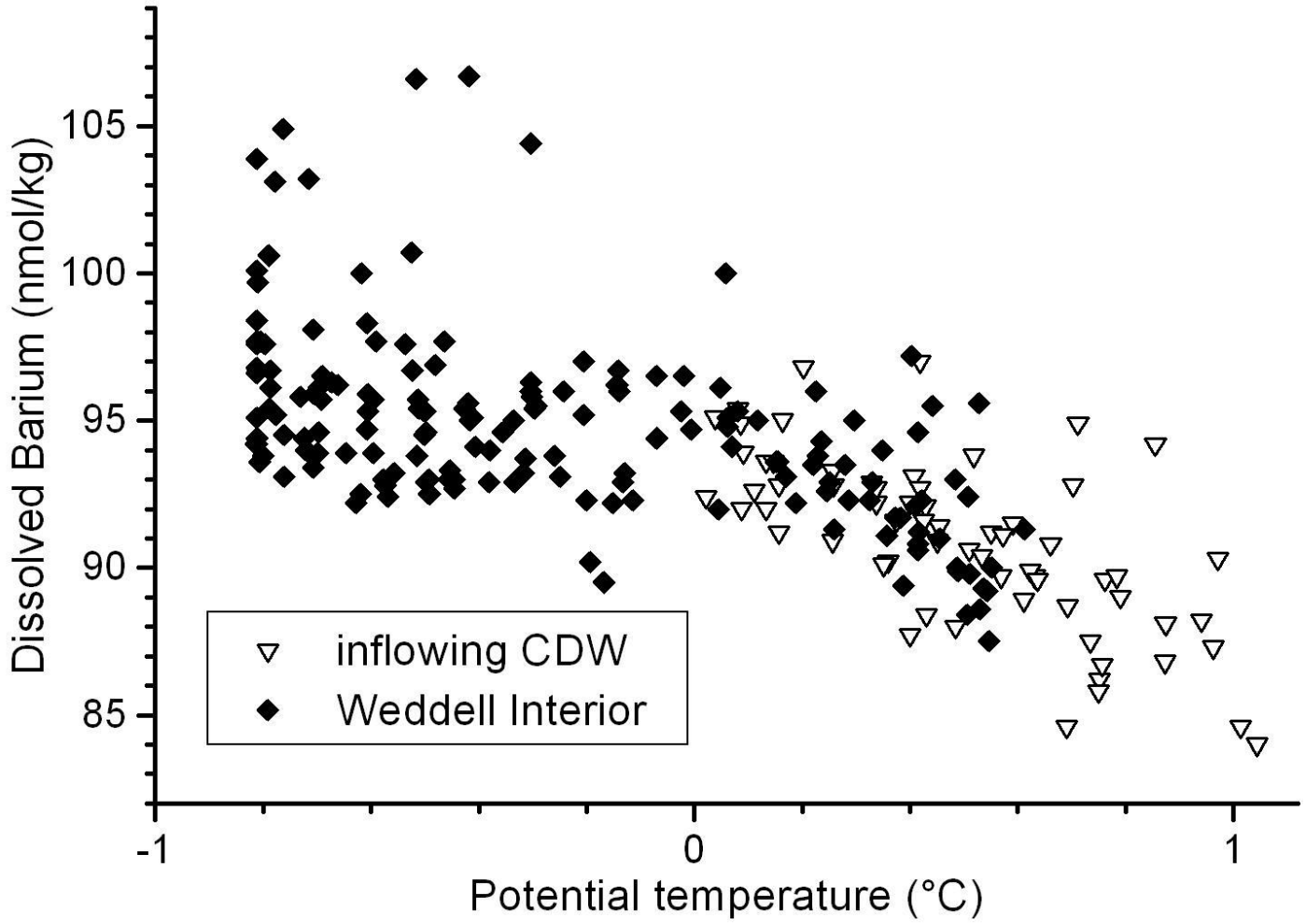
Dissolved Barium (nmol/kg)
105
100
95
90
85
-1
0
1
Potential temperature (°C)
inflowing CDW
Weddell Interior

FIGURE 9